Chemical Vapor Deposition of Metal Fluorides Using Sodium and Zirconium Fluoroalkoxides

John A. Samuels, Wen-C. Chiang, Chung-P. Yu, Elizabeth Apen, David C. Smith, David V. Baxter,* and Kenneth G. Caulton*

Department of Chemistry, Indiana University, Bloomington, Indiana 47405

Received March 4, 1994. Revised Manuscript Received July 14, 1994[⊗]

CVD onto borosilicate glass from $(NaOR_f)_4$ and from $Zr(OR_f)_4$ gives NaF and ZrF_4 films, respectively. Various fluorinated groups $OR_f = OCH(CF_3)_2$ and $OCMe_{3-n}(CF_3)_n$ ($n = 1-3$) are studied, and metal-free fluorocarbon products are analyzed (^1H and ^{19}F NMR spectra) to show that the transfer of F from carbon to metal occurs with 1,2-migration of a group in the alkoxide to the carbon losing the fluorine; such migration is increasingly facile in the order $CF_3 \ll CH_3 \leq H$. Fluorinated ketones or their polymerization products are formed. An analysis of the fragmentation processes of these $(NaOR_f)_4$ and $Zr(OR_f)_4$ molecules under low-energy (15 eV) electron impact also shows stepwise conversion of metal alkoxide to metal fluoride by loss of ketone. Since the $(NaOR_f)_4$ molecules show intramolecular Na/F bonding interactions in the solid state and since these volatilize as tetramers (mass spectral evidence), this is suggested to be the factor which leads to the CVD production of NaF rather than its oxide. However, since there is no solid-state structural evidence for Zr/F interactions in $Zr(OR_f)_4$, a metal as electrophilic as Zr(IV) can display C–F cleaveage even without M/F interactions in its ground-state structure; threshhold temperatures for CVD with $Zr(OR_f)_4$ are higher, however.

Introduction

In the investigation of molecules as precursors to ceramic solids via chemical vapor deposition (CVD), many ligand types and substituents have been utilized. For the production of metal oxides, species such as metal alkoxides and β-diketonates[1] have been utilized in the hope that the metal/oxygen bond found in the precursor will be maintained during processing. This strategy has been successful[1,2] and has allowed researchers to modify the remaining organic portion of the molecule to obtain desired solution and/or gas-phase characteristics, while still producing the oxide products.[3] An exception to this rule is found when fluorine is incorporated into the organic portion of the precursor (as a means of increasing solubility and volatility).[4] These fluorinated systems are usually found to produce metal fluorides instead of metal oxides for both β-diketonate[5]- and alkoxide[6]-based precursors. It is tempting to attribute this simply to thermodynamics, since the metal fluorides are typically more stable than the oxides.[7] However, there exists at least one case where kinetic constraints prevent the system from reaching the most thermodynamically-stable state: CVD of $Zr(TFAC)_4$ produces[8] ZrO_2 not ZrF_4. Even in cases where metal fluorides are formed, the mechanism through which this takes place is unclear since, based on connectivity, the fluorine atoms are at least four bonds away. In this work, we investigate these mechanistic questions more systematically.

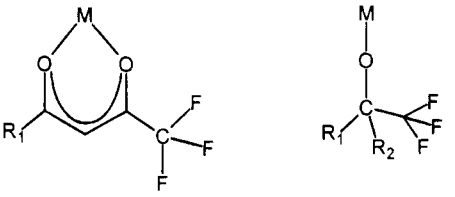

Recently, we reported the observation of close metal–fluorine contacts between monovalent main-group metal ions and fluoroalkoxides both in the solid state and in solution:[9]

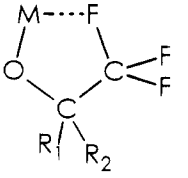

Similar contacts have been observed for divalent and trivalent metal centers for both fluoroalkoxides[10] and fluoro-β-diketonate systems.[11] In contrast, such contacts are lacking in $Zr(OR_f)_4$ species.[9]

[⊗] Abstract published in *Advance ACS Abstracts,* August 15, 1994.

(1) For general reviews, see: (a) Bradley, D. C. *Chem. Rev.* **1989**, *89*, 317. (b) Hubert-Pfalzgraf, L. G. *Appl. Organomet. Chem.* **1992**, *6*, 627.

(2) Xue, Z.; Vaartstra, B. A.; Caulton, K. G.; Chisholm, M. H.; Jones, D. C. *Eur. J. Solid State Inorg. Chem.* **1992**, *29*, 213.

(3) Schulz, D. L.; Hinds, B. J.; Stern, C. L.; Marks, T. J. *Inorg. Chem.* **1993**, *32*, 249.

(4) Bradley, D. C.; Chudzynska, H.; Hursthouse, M. B.; Motevalli, M.; Wu, R. *Polyhedron* **1993**, *12*, 2955.

(5) (a) Purdy, A. P.; Berry, A. D.; Holm, R. T.; Fatemi, M.; Gaskill, D. K. *Inorg. Chem.* **1989**, *28*, 2799. (b) Zhao, J.; Dahmen, K.-H.; Marcy, H. O.; Tonge, L. M.; Marks, T. J.; Wessels, B. M.; Kannewurf, C. R. *Appl. Phys. Lett.* **1989**, *53*, 1750. (c) Larkin, D. L.; Interrante, L. V.; Bose, A. *J. Mater. Res.* **1990**, *5*, 2706.

(6) Lingg, L. J.; Berry, A. D.; Purdy, A. P.; Ewing, K. J. *Thin Solid Films* **1992**, *209*, 9.

(7) $\Delta G°_f$ (kcal/mol): −456.8 (β-ZrF_4), −249.24 (α-ZrO_2), −129.902 (NaF), −89.74 (Na_2O). See: *Handbook of Chemistry and Physics*, 66th ed.; Weast, R. C., Ed.; CRC Press Inc.: Boca Raton, FL; pp D51–93.

(8) Balog, M.; Schieber, M.; Michman, M.; Patai, S. *J. Electrochem. Soc.* **1979**, *126*, 1203.

(9) Samuels, J. A.; Lobkovsky, E. B.; Streib, W. E.; Folting, K.; Huffman, J. C.; Zwanziger, J. W.; Caulton, K. G. *J. Am. Chem. Soc.* **1993**, *115*, 5093.

0897-4756/94/2806-1684$04.50/0

Table 1. Chemical Characteristics

	sublimation temp (10^{-2} Torr)	NMR (ppm) ^1H[a]	NMR (ppm) ^{19}F[b]
Na(HFIP) (**1a**)	80	4.12[c] (sept, $^3J_{H-F}$ = 6.5 Hz)	−83.4[c] (d, $^3J_{H-F}$ = 6.5 Hz)
Na(TFTB) (**1b**)	120	1.05(5)[d]	−85.9(5)[d]
Na(HFTB) (**1c**)	100	1.41(5)[c]	−85.1(5)[c]
Na(PFTB) (**1d**)	30		−81.1(5)[c]
$Zr(HFIP)_4$ (**2a**)	70	4.79[c] (br, sept, $^3J_{H-F}$ = 5.4 Hz)	−77.3 (br, s)[c]
$Zr(TFTB)_4$ (**2b**)	*e*	1.25(5)[d]	−84.9(5)[d]
$Zr(HFTB)_4$ (**2c**)	40	1.54(5)[c]	−82.9(5)[c]
$Zr(PFTB)_4$ (**2d**)	35		−77.9(5)[c]
$Na_2Zr(HFIP)_6$ (**3**)	110	4.63[c] (br sept, $^3J_{H-F}$ = 3.7 Hz)	−80.2[c] (br, sept, $^3J_{H-F}$ = 3.7 Hz)

[a] Internal or external reference to residual protons in C_6D_6 = 7.15 ppm. [b] External reference F_3CCOOH (neat) = −78.45 ppm. [c] Solvent = C_6F_6. [d] Solvent = C_6D_6. [e] Liquid at room temperature distilled at 60 °C and 10^{-2} Torr.

We report here comparative CVD studies of $[Na(OR_f)]_4$[9] and $Zr(OR_f)_4$ as a means of understanding the influence which these intramolecular M−F interactions may have on the deposition behavior of the precursor. These investigations also explore the impact of systematic chemical modification (by fluorine incorporation) of the group R_f in the zirconium and sodium systems.

We have also attempted to learn something about the reactivity of these molecules in the gas phase under "intermediate energy" conditions by analysis of their electron impact mass spectra (MS). The combination of CVD and MS results provide evidence for a mechanism for metal−fluoride formation from these fluoroalkoxide species.

Experimental Section

All manipulations were carried out under dry nitrogen atmosphere using oven-dried glassware. Solvents were freshly distilled over Na/benzophenone. Reagents were purchased from Aldrich with the exception of fluorinated alcohols which were purchased from PCR. Tetraneopentyl zirconium,[12] zirconium *tert*-butoxide,[13] and $Na_2Zr(HFIP)_6$[9] were prepared by literature methods. $Na(OR_f)$ (**1a**−**d**) and $Zr(OR_f)_4$ (**2a**−**d**) were synthesized from the parent alcohol and NaH or $Zr(NP)_4$ via literature methods.[9] Physical and spectroscopic characteristics are reported in Table 1. NMR spectra were run on a Nicolet NT-360 spectrometer (^{19}F, ^1H, spectra at 340 and 361 MHz, respectively). Samples were run in C_6D_6 and C_6F_6 with external references when necessary (F_3CCOOH (neat) = −78.45 ppm, ^1H residual protons in C_6D_6 = 7.15 ppm). NMR signal intensities are quoted relative to the highest peak in the spectrum. Infrared spectra were run on a Nicolet 510P FT-IR spectrometer as KBr pellets. Elemental analyses were performed by Oneida Research Services. Abbreviations: OR_f = general fluorinated alkoxide, HFIP = hexafluoroisopropoxide ($OCH(CF_3)_2$), TFTB = trifluoro-*tert*-butoxide ($OCMe_2(CF_3)$), HFTB = hexafluoro-*tert*-butoxide ($OCMe(CF_3)_2$), PFTB = perfluoro-*tert*-butoxide ($OC(CF_3)_3$). Substrates for CVD studies consist of borosilicate microscope slides prepared by washing in isopropanol followed by a 30 min rinse in deionized water. Substrates were stored in an oven at 100 °C. The quoted deposition temperatures produced deposits near the center of the furnace, where the thermocouple was located. The temperature at the furnace exits was within 10 °C of that at the furnace center.

X-ray photoelectron spectroscopy (XPS) analysis was executed in a spectrometer with base pressure of 10^{-10} Torr using Mg Kα radiation and a standard hemispherical analyzer with a pass energy of 20 eV. Typical data collection time was 15 min for a 20 eV scan. The C 1s, O 1s, F 1s, and Zr 3d regions were monitored at a sample temperature of 25 °C. The films were first cleaned in vacuum for 5 min with a 3 keV Kr^+ sputter beam with a background Kr pressure of 5×10^{-5} Torr. A ZrF_4 pressed pellet (0.25 mm thick) showed preferential removal of F atoms during sputtering, so spectra from the unsputtered standard were used with published literature sensitivity values to calculate atom ratios in the CVD films. For the estimation of atom ratios in the films, a secondary electron background was first subtracted from the raw data using a smoothed step function.[14] Integrated peak areas were then calculated for each region. Using literature sensitivity values,[15] relative concentrations were then calculated and normalized to the ZrF_4 standard.

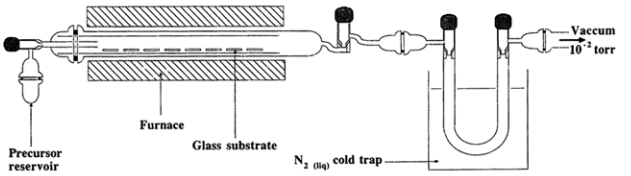

Figure 1. Schematic diagram of chemical vapor deposition apparatus used in thermal conversion of fluoroalkoxides.

Table 2. Chemical Vapor Deposition Conditions and Solid-State Products

precursor	source temp (°C)	furnace temp (°C)	product
Na(HFIP) (**1a**)	75	255	NaF
Na(TFTB) (**1b**)	100	260	NaF
Na(HFTB) (**1c**)	80	300	NaF
Na(PFTB) (**1d**)	90	400	NaF
$Zr(TFTB)_4$ (**2b**)	30	375	ZrF_4
$Zr(HFTB)_4$ (**2c**)	30	450	ZrF_4
$Zr(PFTB)_4$ (**2d**)	30	460	"ZrF_4"
$Na_2Zr(HFIP)_6$ (**3**)	100	255	Na_3ZrF_7

CVD Using $Na(OR_f)$. $Na(OR_f)$ (0.50 g) was loaded into a glass sample chamber and attached to a glass reactor chamber containing prepared glass plate substrates and fitted with a cold trap downstream (see Figure 1 for diagram). The system was evacuated to 10^{-2} Torr, and the reactor heated to deposition temperature (Table 2) for 1 h to remove any moisture. The cold trap was then filled with N_2(l) and the sample chamber was heated to precursor sublimation temperature where, over a period of 6 h, $NaOR_f$ sublimed and an off-white iridescent coating was deposited in the reactor chamber. This coating was found to adhere poorly to the substrates for all precursor compositions. Upon completion of the deposition, the contents of the cold trap were vacuum transferred to a NMR tube containing benzene-d_6. Chemical shifts (ppm) and relative signal intensities for volatiles: **1a** oil: ^{19}F NMR (THF-

(10) Purdy, A. P.; George, C. F. *Inorg. Chem.* **1991**, *30*, 1970. Labrize, F.; Hubert-Pfalzgraf, L. G.; Daran, J.-C.; Halut, S. *J. Chem. Soc., Chem. Commun.* **1993**, 1556.
(11) (a) Hubert-Pfalzgraf, L. G.; Massiani, M. C.; Papiernik, R.; Poncelet, O. *J. Phys.* **1989**, *50*, C5−981.
(12) Davidson, P. J.; Lappert, M. F.; Pearce, R. *J. Organomet. Chem.* **1973**, *57*, 269.
(13) Thomas, I. M. *Can. J. Chem.* **1961**, *39*, 1386.
(14) Shirley, D. A. *Phys. Rev. B* **1972**, *5*, 4709.
(15) Muilenberg, G. E., Ed. *Handbook of X-ray Photoelectron Spectroscopy*; Perkin-Elmer Corp.: Eden Prairie, MN, 1979.

d_8) −65.2 (br, 10%); −66.7 (br, 10%), −74.5 (br, 30%), −75.0 (br, 50%), −78.2 (d, $^3J_{HF}$ = 6.5 Hz, NaHFIP, 5%), −225.1 (br, 5%). ^{1}H NMR (THF-d_8) 6.8 (5%), 6.7 (5%), 6.4 (br), −74.8 (d, J = 5.8 Hz, 5%), −76.7 (d, $^3J_{H-F}$ = 5.1 Hz, H-HFIP, 70%); ^{1}H NMR (benzene-d_6) 5.38 (sept, J = 5.8 Hz, 5%), 5.18 (sept, J = 5.7 Hz, 5%), 3.35 (sept, $^3J_{H-F}$ = 5.1 Hz, H-HFIP, 70%), 2.09 (br, 20%), 1.92 (sept, J = 9.5 Hz, 10%).

Transferable Trap Contents. 1b: ^{19}F NMR (benzene-d_6) −71.3 (60%), −76.1 (d, J = 10 Hz, 15%), −76.4 (d, J = 10 Hz, 10%), −84.8 (H-TFTB, 100%, −132.8 (15%). ^{1}H NMR (benzene-d_6) 5.15 (10%), 4.65 (sept, J = 1.5 Hz, 10%), 3.58 (10%), 1.57 (100%), 1.46 (10%), 1.23 (10%), 1.06 (H-TFTB, 75%), 0.85 (10%).

1c: ^{19}F NMR (benzene-d_6) −63.5 (d of d, J = 11.5 Hz, 23 Hz, 10%), −64.7 (10%), −65.8 (50%), −70.1 (35%), −70.2 (d, J = 7 Hz, 60%), −70.3 (15%), −74.5 (10%), −77.0 (15%), −79.9 (H-HFTB, 100%), −80.7 (15%), −132.7 (3%), −163.7 (3%). ^{1}H NMR (benzene-d_6) 5.37 (20%), 2.58 (10%), 1.51 (H-HFTB, 100%), 1.40 (10%), 1.14 (5%), 1.11 (10%), 1.09 (20%), 1.04 (10%).

1d: See ref 9.

CVD Using Zr(OR$_f$)$_4$. Zr(OR$_f$)$_4$ (0.50 g) was deposited (Table 2) using the identical procedure as for Na(OR$_f$) (above). The resulting colorless films are found to adhere well to the substrate for all precursor compositions.

Chemical shifts (ppm) and relative signal intensities for transferable volatiles:

2b: ^{19}F (benzene-d_6) −84.8 (H-TFTB, 80%), −100.6 (quart, $^3J_{F-H}$ = 19 Hz, 100%), −146.1 (5%), −247.3 (d, J = 16 Hz, 5%), −251.4 (15%). ^{1}H (benzene-d_6) 5.80 (15%), 5.13 (10%), 1.80 (t, $^4J_{H-F}$ = 2.4 Hz, 50%), 1.50 (d, J = 2.1 Hz, 20%), 1.35 (10%), 1.28 (10%), 1.28 (t, $^3J_{H-F}$ = 19 Hz, 50%), 1.12 (5%), 1.06 (H-TFTB, 80%).

2c: ^{19}F (benzene-d_6) −66.0 (10%), −70.2 (d, J = 7.8, 3%), −70.4 (d, J = 4 Hz, 3%), −74.7 (d, J = 13 Hz), −80.0 (30%), −80.6 (H-HFTB, 100%), −132.7 (10%), −163.7 (10%). ^{1}H (benzene-d_6) 5.42 (5%), 1.56 (H-HFTB, 100%), 1.08 (mult, 10%), 1.02 (d, J = 3 Hz, 15%).

2d: ^{19}F (benzene-d_6) −70.5 (t, J = 8 Hz, 75%), −71.8 (br, 50%), −76.7 (H-PFTB, 100%), −78.3 (br, 40%), −78.9 (HCF$_3$, d, $^2J_{F-H}$ = 79 Hz, 10%), −83.6 (10%), −109.6 (mult, 10%), −164.0 (10%). ^{1}H (benzene-d_6) 5.26 (HCF$_3$, quart, $^2J_{F-H}$ = 79 Hz, 33%), 2.61 (5%), 2.38 (H-PFTB, 100%).

CVD Using Zr(TFTB)$_4$/Zr(O^t-Bu)$_4$. Zr(TFTB)$_4$ (*2b*, 0.15 g, 0.25 mmol) Zr(O^t*Bu*)$_4$ (0.10, 0.25 mmol) were combined in a source chamber. The source was heated to 30 °C with the reactor furnace at 375 °C. A homogeneous light tan film was deposited over 6 h which had poor adhesion. Analysis by powder X-ray diffraction indicated that the film consisted of ZrO_2.

CVD Using Na$_2$Zr(HFIP)$_6$ (3). Na$_2$Zr(HFIP)$_6$ (0.50 g) was deposited (Table 2) using the identical procedure as for Na(OR$_f$) (above). The resulting colorless films adhere poorly to the substrate. Chemical shifts (ppm) and relative signal intensities for volatiles: oil: ^{19}F (THF-d_8) −75.1 ppm (br, 50%), −77.6 (d, $^3J_{H-F}$ = 6 Hz, Zr(HFIP)$_4$, 100%), −77.7 (d, $^3J_{H-F}$ = 5 Hz, *3*, 90%). ^{1}H (THF-d_8) 6.96 (10%), 4.81 (sept, $^3J_{H-F}$ = 6 Hz, 100%), 4.70 (sept, $^3J_{H-F}$ = 5 Hz, 90%), 4.86 (br, 30%), 1.72 (5%). Trap: ^{19}F (benzene-d_6) −58.8 (mult, 5%), −64.5 (mult, 10%), −65.0 (d, J = 7 Hz, 5%), −74.9 (d, 6 Hz, 10%), −76.7 (d, $^3J_{H-F}$ = 5.1 Hz, H-HFIP, 100%), −83.5 (5%), −175.9 (10%). ^{1}H (benzene-d_6) 5.20 (mult, 10%), 4.0−3.8 (multiplets, 10% total), 3.35 (sept, $^3J_{H-F}$ = 9.5 Hz), 0.89 (mult, 30%).

Results

Mass Spectrometric Analysis. Mass spectral formation via electronic ionization has been shown to mimic thermolysis pathways.[16] Thus, to gain information on degree of oligomerization in the gas phase and possible mechanisms of decomposition, mass spectra were obtained on species **1a**−**d**, **2a**−**d**, and **3**. Samples were sublimed into the mass spectrometer where they were ionized via electron bombardment. Low ionization energy was used (usually 15−30 eV) to minimize fragmentation.[17]

Scheme 1

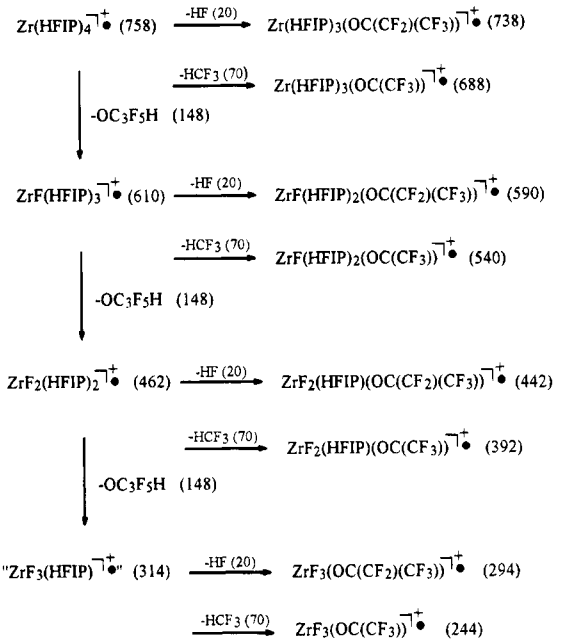

The mass spectra of the Na(OR$_f$) species at 15 eV revealed no parent ion, even at these low ionizing voltages. The most abundant ions were the products of the elimination of anions from the oligomers. The highest mass of significant population observed for most of the systems corresponds to $[Na_4(OR_f)_3]^+$, the product of the explusion of OR_f^- from the tetrameric framework. Lower concentrations of $[Na_5(OR_f)_4]^+$ and $[Na_6F(OR_f)_4]^+$ were detected for species **1a** and, at higher sample temperatures, for **1c**. Electron impact ejection of larger anionic clusters from $[Na(OR_f)]_4$ was also apparent given the presence of $[Na_3(OR_f)_2]^+$ and $[Na_2(OR_f)]^+$. These fragmentation patterns are similar to those observed in other $[M^I(OR)]_4$ species.[18a,b] It is important to note that metal fluorides were observed in appreciable amounts as $[Na_4F(OR_f)_2]^+$ and $[Na_2F]^+$. This implies that metal−fluoride formation can occur intramolecularly, a trait observed in other fluorine-containing metal species.[18c,d] An increase of ionization energy from 15 to 30 eV resulted in no significant change in the mass spectral cracking pattern.

An examination of **2a**[19] at 15 eV did reveal a parent ion peak of 758 amu, which would indicate that the homometallic zirconium fluoroalkoxide ion has greater stability than **1** or **3**. On the basis of the observed ion peaks,[17] the following cracking pattern shown in Scheme 1 is proposed (species in quotes were not observed and masses are for the ^{90}Zr isotope). Numerous zirconium-free fluorocarbon ions were observed in the lower mass

(16) *Spectroscopic Identification of Organic Compounds*, 3rd ed.; Silverstein, R. M., Bassler, G. C., Morrill, T. C., Eds.; John Wiley and Sons: New York, 1974; Chapter 2.

(17) (a) Tables of observed masses and intensities for metal-containing fragments are available as supplementary material. (b) Numerous metal-free ions were detected for all species.

(18) (a) Weiss, E.; Alsdorf, H.; Kuhr, H.; Grutzmacher, H. F. *Chem. Ber.* **1968**, *101*, 3777. (b) Hartwell, G. E.; Brown, T. L. *Inorg. Chem.* **1966**, *5*, 1257. (c) Reichert, C.; Westmore, J. B.; Gesser, H. D. *J. Chem. Soc., Chem. Commun.* **1967**, 782. (d) Clobes, A. L.; Morris, M. L.; Koob, R. D. *J. Am. Chem. Soc.* **1969**, *91*, 3087.

(19) Mazdiyasni, K. S.; Schaper, B. J.; Brown, L. M. *Inorg. Chem.* **1971**, *10*, 889.

Scheme 2

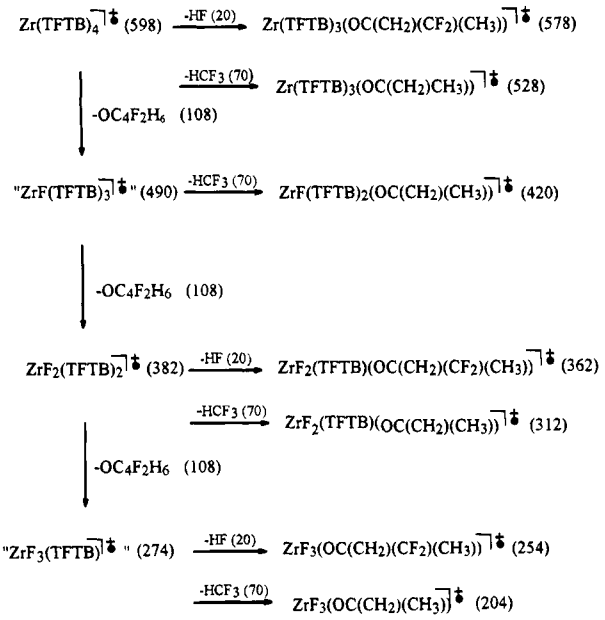

range. The observed elimination of HF and HCF_3 is common in mass spectra of hydrofluorocarbons.[20] The apparent formation of metal fluoride species is the result of the repeated loss of an OC_3F_5H molecule:

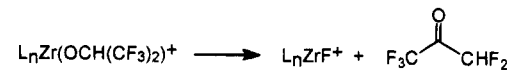

Arguments for the identity of this molecule as pentafluoropropan-2-one will be discussed later.

The mass spectrum of $Zr(TFTB)_4$ (**2b**) at 15 eV also showed a parent ion peak (598 amu). On the basis of the observed ions[17] and the observations for other $Zr(OR_f)_4$ species, the cracking pattern shown in Scheme 2 is proposed. Although some species (in quotes) were not observed, their analogues were detected for **2a**. Similar to **2a**, there is evidence for the production of metal fluorides via the repeated loss of $OC_4F_2H_6$. A possible identity for this species is 3,3-difluorobutan-2-one. Compound **2b** does not appear to lose HF as easily as does **2a**. This is due to the lack of protons on the carbon α to the CF_3 group (unlike **2a**):

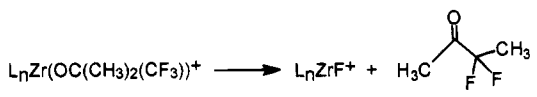

The mass spectrum of $Zr(HFTB)_4$ (**2c**) at 15 eV showed a parent ion peak at 814 amu's. From the lower mass ions observed,[17] the cracking pathway shown in Scheme 3 is proposed. As with the previous two examples, the repeated loss of a neutral species appears to produce metal fluorides. In this case, $OC_4F_5H_3$ is proposed to be 1,1,1,3,3-pentafluorobutan-2-one:

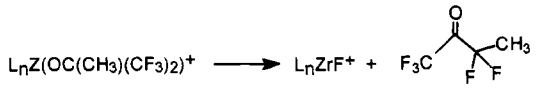

Here for the first time, HF is eliminated from species which have already eliminated HCF_3. This may be the result of the higher fluorine content of the ligand as compared to the other fluoroalkoxy species.

Scheme 3

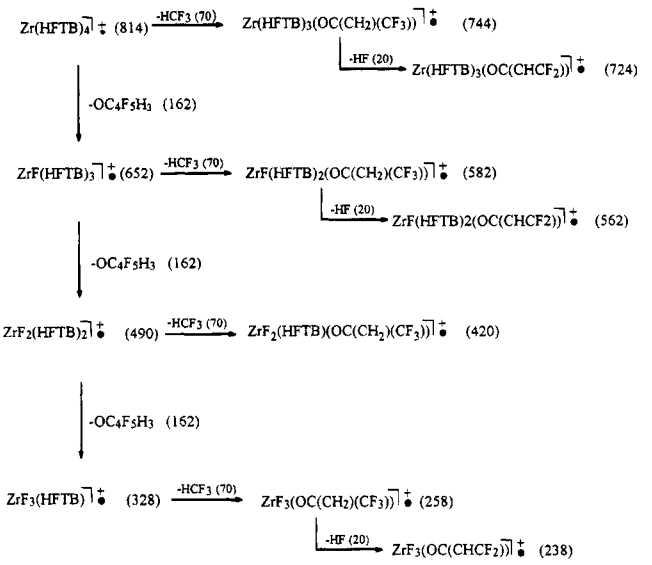

For **2d** ($Zr(PFTB)_4$), a much simpler spectrum is observed.[17] No parent ion is detected with the largest mass being 1011 amu, corresponding to the elimination of an F^- from the molecular species. Peaks attributed to $Zr(PFTB)_3^+$ (795 amu) and $ZrF(PFTB)_2^+$ (579 amu), as well as numerous low- and medium-mass fluorocarbon ions were observed. The spectroscopic simplicity for **2d** as compared to the other $Zr(OR_f)_4$ species may be due to the lack of protons on the ligands, removing various mechanistic pathways present in the previous species.

For the mixed-metal complex **3** the mass spectra[17] at 30 eV were similar to those of **1a–d**, in that no parent ion peak is detected and the main form of fragmentation is the loss of anionic units to yield $[Na_2Zr(OR_f)_5]^+$, $[NaZr(OR_f)_4]^+$, and $[Na_2(OR_f)]^+$. Also present were metal fluorides in the form $[Na_2ZrF(OR_f)_4]^+$, $[Na_2ZrF_2(OR_f)_3]^+$, and $[Na_2F]^+$. As for **1a** and **1c**, **3** did produce significant amounts of higher molecular weight species $[Na_3ZrF(OR_f)_5]^+$, $[Na_3ZrF_2(OR_f)_4]^+$, $[Na_3Zr(OR_f)_6]^+$, and $[Na_4Zr(OR_f)_7]^+$ at all sample temperatures. This would indicate the possibility of either higher oligomers of these heterometallics in the gas phase or that recombination of various molecular fragments is occurring in the mass spectrometer. Only minimal amounts of metal-free ions were detected.

It is interesting to note the fundamental difference between the ionization patterns seen for the sodium and zirconium species. In the sodium systems, primary ionization appears to occur via even-electron species; no radicals appear to be formed. In the case of the zirconium species, ionization does occur via expulsion of a single-electron-giving radical species. A possible explanation is that the zirconium species, having terminal alkoxides with oxygen lone pairs, have HOMOs of higher energy than those of the sodium alkoxide cubes:

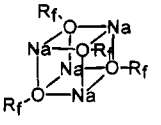

(20) Majar, J. R. *Adv. Fluorine Chem.* **1961**, *2*, 55.

where all the oxygen lone pairs are involved in bonding. Thus it is easier to remove an electron and produce a radical from the zirconium than from the sodium fluoroalkoxide species. For the sodium system, bond cleavage and ligand expulsion is a lower energy process. This trend appears to hold for the heterometallic systems as well, because all alkoxide oxygens are bridging.[9]

Chemical Vapor Deposition: General Methods. To observe the effects of fluorination of alkoxides on the deposition of inorganic material, CVD studies were performed on the homometallic species, as well as **3**. The Pyrex apparatus (Figure 1) consisted of an independently-heated source chamber, a hot-walled reactor containing glass plate substrates where deposition takes place, and a liquid nitrogen trap downstream from the reactor to collect the volatile products for later analysis. The overall system was evacuated to 10^{-2} Torr. Table 2 shows the minimum temperature for sublimation at a practical rate. The reactor was heated to the lowest temperature at which a minimum of precursor sample passes through the furnace unchanged (Table 2). Over the course of 6 h, coatings were deposited on the reactor walls and the glass substrates. Adhesion of the films was tested by applying cellophane tape to the coated substrate and observing if the film was removed by the tape. Analysis of the deposited solid was conducted via powder X-ray diffraction. Bulk elemental analysis was performed on the sodium-containing films which were easily removed from the substrate.

(a) [Na(OR$_f$)]$_4$. *CVD using **1a** (Table 2)*: Chemical vapor deposition using **1a** at 255 °C produced very light tan transparent films on the substrates. These films were found to adhere very poorly to the substrates, a characteristic common to all the Na(OR$_f$) deposition products studied. X-ray diffraction of the films indicated the presence of randomly oriented NaF, which is consistent with previous reports.[6,9] Bulk elemental analysis confirmed this result with samples consisting of >98% NaF (0.5% C). For **1a**, the volatiles from the deposition reaction were isolated downstream of the reactor in two phases, a viscous amber oil just outside of the hot zone, and a colorless liquid in the liquid nitrogen trap. The viscous oil was found to be insoluble in aromatic solvents. Fluorinated solvents were avoided due to potential interference with NMR analysis. However, the oil was completely soluble in THF-d_8. The ^{19}F NMR spectrum indicates that the oil is a mixture of products containing (ca. 5%) unreacted **1a**. The other components of the mixture produce four broad signals (210−360 Hz) in the region of aliphatic $-CF_3$ groups (95% of F intensity), and one very broad peak (600 Hz half-height, ca. 5%) falling in the region for fluorine attached to either olefinic or tertiary carbons.[21] The ^{1}H NMR spectrum of the oil shows signals for unconverted **1a** together with major peaks at 6.4 and 5.5 ppm (also very broad and ca. 30% and 50%, respectively). These signals are consistent with highly deshielded protons, possibly due to fluorine inductive effects. Minor products are observed at 6.8 and 6.7 ppm (ca. 5% each). There is evidence of some vinylic material being present, based on both the proton and fluorine spectral data, but this material is only a minor component (ca. 10% total). Given the limited fine structure of both spectra, little can be concluded about the major products except that the broad nature of the signals, as well as the oily physical appearance of the material, suggests a polymeric material with both fluorine- and proton-containing units.

The contents of the liquid nitrogen trap were vacuum transferred to an NMR tube containing C_6D_6. The ^{19}F NMR spectrum indicates that the main product is hexafluoroisopropyl alcohol (ca. 70%). The other 30% is made up of at least nine other trace signals appearing as doublets. The proton NMR spectrum confirms that the alcohol is the major product among a variety of other complex signals ranging from 5.5 to −0.1 ppm.

*CVD using **1b***: CVD using **1b** at 260 °C produced films similar to those formed from **1a** although somewhat darker in appearance. X-ray powder pattern analysis indicated that this material consisted of randomly oriented NaF, and this identity was confirmed by bulk elemental analysis (>97% NaF, 0.9% C). Unlike **1a**, **1b** did not produce any oily material as part of the deposition volatiles. Vacuum transfer of the contents of the liquid nitrogen trap produced a colorless liquid. The ^{19}F NMR spectrum of this material in benzene-d_6 showed a signal corresponding to the parent alcohol as the major product, as well as a signal at −71.3 ppm (60%, CF_3 groups),[21] plus numerous other low-intensity peaks. The ^{1}H NMR spectrum confirms the presence of the alcohol, as well as a second major product at 1.37 ppm. Numerous other low-intensity signals were observed. The large number of NMR signals would seem to indicate either numerous products or at least two or three products with a highly complex structure. It should be noted that the analysis techniques do not preclude the possibility of secondary reactions occurring among the deposition volatiles in either the cold trap or the NMR tube itself.

*CVD using **1c***: CVD using **1c** at 300 °C produced a light tan transparent film which, by X-ray diffraction, was found to consist of randomly oriented NaF. This was confirmed by elemental analysis which also indicated the film was contaminated with 1.5% carbon. Upon warming the deposition volatiles for vacuum transfer, the colorless liquid rapidly transformed to a brown, nonvolatile oil, indicating the occurrence of secondary reactions. The ^{19}F NMR spectrum of the material which did transfer was very complex, with numerous low-intensity signals ranging from −63 to −164 ppm. The parent alcohol was the primary ^{19}F NMR signal. The ^{1}H NMR spectrum is also fairly complex, with numerous signals from 5.37 to 1.09 ppm, and the primary signal corresponding to the parent alcohol. Unfortunately, due to the occurrence of secondary chemical reactions, in conjunction with the complexity of the volatile mixture spectra, identification of the volatiles was not possible.

*CVD using **1d***: Our results were consistent with previous reports of the CVD using Na(PFTB), **1d**.[6] This material requires deposition temperatures of 400 °C and produces randomly oriented NaF films. The main volatile product observed was the parent alcohol.[6]

(b) Zr(OR$_f$)$_4$. *CVD using **2a***: The CVD using Zr(HFIP)$_4$ (**2a**) required temperatures in the regions of 450 °C for precursor conversion. Unfortunately, under these conditions, the films were of such poor quality that analysis by powder diffraction was impossible.

*CVD using **2b***: The CVD using Zr(TFTB)$_4$ (**2b**) produced a pure white film with excellent adhesion at

(21) Emsley, J. W.; Phillips, L. *Prog. NMR Spectrosc.* **1971**, *7*, 1.

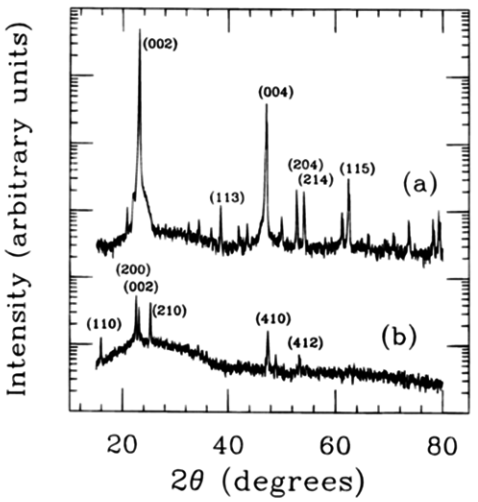

Figure 2. X-ray diffraction patterns (Cu Kα radiation, glass substrate) of films produced by CVD processing of species **2b** at (a) 400 °C and (b) 375 °C. Both films consists of β-ZrF_4 but pattern (a) indicates a highly oriented (002) film. Curve (a) has been offset vertically for clarity.

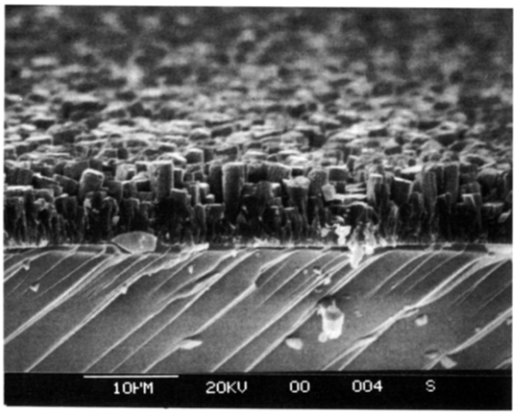

(A)

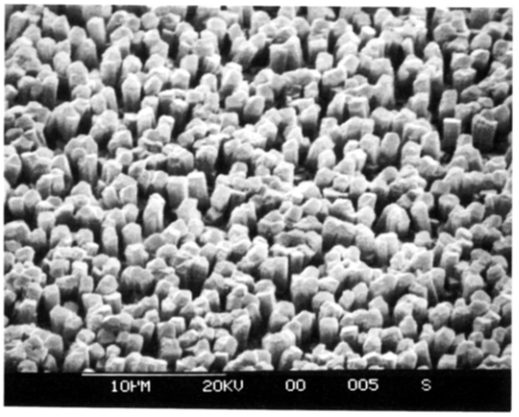

(B)

Figure 3. SEM images of the thin film produced via CVD of $Zr(TFTB)_4$ (**2b**) at 400 °C.

375 °C. The film was found to consist of randomly oriented β-ZrF_4. By increasing the deposition temperature to 400 °C, a ⟨002⟩ oriented film was produced (Figure 2). Scanning electron micrographs (SEM, Figure 3) indicated that the substrate was coated on both sides. The material consisted of a uniform 4−5 μm thick film of crystallites. Image A shows a cross section of the film where the substrate was cut. The oriented crystallites can be seen to taper toward their base, with the film having increasing density as one approaches the substrate. Image B is a view perpendicular to the

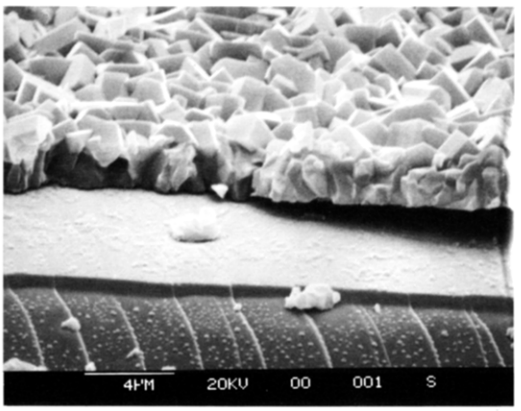

(A)

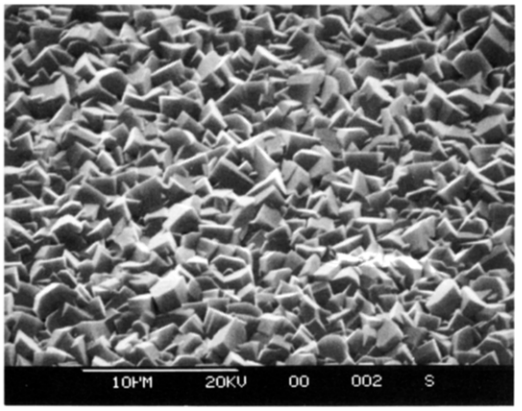

(B)

Figure 4. SEM images of the thin film produced via CVD of $Zr(HFTB)_4$ (**2c**) at 450 °C.

film showing the ⟨002⟩ face of the crystallites. From this image, the size of the crystallites appears to be roughly uniform at approximately 750 nm. Carbon and oxygen impurities were found at 3.6 and 5.4 atom % by XPS.

The ^{19}F NMR spectrum of the volatiles from the deposition showed signals at for the parent alcohol, and a quartet at −100.6 ppm (J_{F-H} = 19 Hz) which corresponds to 3,3-difluorobutan-2-one, in a 0.67:1 mole ratio. Also present are signals corresponding to CF_2 and CF groups.[21] The ^1H NMR spectrum is consistent with the fluorine spectrum, showing the presence of H-TFTB (1.06 ppm) and the ketone species (1.80, t, $^4J_{H-F}$ = 2.4 Hz, 1.28, t, $^3J_{H-F}$ = 19 Hz) also in a 0.67:1 mole ratio. Also observed are various low-intensity signals from 5.8 to 1.12 ppm.

CVD using ***2c***: The CVD using $Zr(HFTB)_4$ (**2c**) required furnace temperatures of 450 °C for complete conversion of the precursor species. The light-gray film that was produced showed good adhesion to the substrate. Powder X-ray diffraction indicated that the film consists of randomly oriented β-ZrF_4. SEM images of the film (Figure 4) indicate that the substrate was coated on both sides. Image A is a cross section of the sample where the substrate was cut. It shows shows that material to be a dense polycrystalline film, 2−3 μm thick. Image B, perpendicular to the film, shows the random nature of the crystallites in both size and orientation. In XPS comparison to a ZrF_4 standard, the film had a composition $ZrF_{3.9}$. Carbon and oxygen impurities were found at 6.5 and 4.0 atom %.

Upon warming the volatiles for vacuum transfer, rapid discoloration occurred, producing a dark brown involatile oil similar to that observed for Na(HFTB)

(above). The ^{19}F NMR spectrum of the material which remained volatile showed signals for the parent alcohol as the major component, as well as numerous peaks corresponding to CF_3 and CF_2 groups. The ^1H NMR spectrum confirmed the presence of the alcohol as a major component of the mixture, as well as numerous low-intensity peaks making up only a fraction of the overall protons present (~30%). Although many of the NMR signals match between the deposition products of **2c** and **1c**, this may mean only that the byproducts of the secondary reactions are the same and not that both systems undergo the same deposition mechanism.

*CVD using **2d**.* The CVD using $Zr(PFTB)_4$ required temperatures in excess of 460 °C for complete conversion. The resulting thin white film was found to have the same characteristics (adhesion and physical appearance) as those from the deposition of **2b** and **2c**. Powder X-ray diffraction pattern (supplementary material; see paragraph at end of paper) is weak, but matches that of ZrO_2. XPS of the film, however, revealed high levels of contaminants (e.g., 7.1 atom % C, 22.8 atom % O) and, in comparison to a ZrF_4 standard, a composition $ZrF_{3.4}$. Attempts to vacuum transfer the deposition volatiles produced a dark brown involatile oil on warming from −196 °C. The ^{19}F NMR of the material that did transfer showed that it consisted primarily of parent alcohol in combination with moderate amounts of HCF_3 and various unidentified fluorine-containing species. ^1H NMR confirmed the presence of the alcohol and HCF_3, as well as other minor products. It is important to note the production of hydrogen-containing species from a hydrogen-free precursor. This indicates an external source of this element (see discussion).

*CVD using **2b** and $Zr(O^tBu)_4$.* To gain information as to the effect of simultaneous deposition of a fluoride-producing and an oxide-producing precursor, a 1:1 mole ratio of the liquid $Zr(TFTB)_4$ and $Zr(O^tBu)_4$ was combined in a CVD reaction source chamber and deposited at 375 °C.[22] This produced a uniform light tan film with poor substrate adhesion. X-ray diffraction of the film indicated the presence of zirconium oxide, though the exact phase could not be determined due to the breadth of the lines. What is most remarkable is the absence of lines corresponding to ZrF_4, even though $Zr(TFTB)_4$ has been shown to deposit metal fluorides at this temperature. The cause of this apparent selectivity of metal oxide over metal fluoride formation is currently under investigation.

*CVD using **3**.* The CVD using $Na_2Zr(HFIP)_6$ was effective at 255 °C, producing a tan transparent film with poor adhesion characteristics. X-ray diffraction indicated that the film consisted of randomly oriented Na_3ZrF_7. Bulk elemental analysis shows the material to contain 3.14% C. The presence of the Na_3ZrF_7 phase indicates a change of Na:Zr stoichiometry during deposition. It is also interesting to note that the deposition temperature is comparable to that of $[Na(HFIP)]_4$ and is much lower than that of the $Zr(OR_f)_4$ precursors (see Discussion). As with $[Na(HFIP)]_4$, an amber oil deposits just downstream of the furnace and a colorless liquid collects in the −196 °C trap. ^{19}F NMR spectrum of the oil in THF-d_8 showed a surprisingly simple pattern with a broad signal at −75.1 ppm (50% relative intensity) and doublets at −77.6 (J = 6 Hz) (100%) and −77.7 (J = 5 Hz, 90%). The doublets are due to $Zr(HFIP)_4$ (**2a**, consistent with the production of Na_3ZrF_7) and unreacted $Na_2Zr(HFIP)_6$ (**3**), respectively. This was confirmed by spectroscopic analysis of a second sample of the oil in C_6F_6; these duplicate the values in Table 1. Proton NMR spectra in THF-d_8 showed signals of **2a** and **3**, as well as signals at 6.96 (10%), 4.86 (broad, 30%), and 1.72 (5%) ppm. ^{19}F NMR spectra of the cold-trap contents in benzene-d_8 indicated the primary product to be the parent alcohol. The proton NMR spectrum shows the signal for the parent alcohol, as well as multiplets at 5.20 (10%), 0.89 (30%), and at 3.8 to 4.0 (10% total intensity) ppm. Although the physical appearances of the volatiles of the deposition of **3** and **1a** are similar, the spectroscopic character was significantly different. This indicates that the heterometallic nature of the precursor can have an effect on the deposition pathway.

(22) The choice of temperature was based on the observation that both precursors readily thermolyse under these conditions.

Discussion

Volatile Products. We interpret the broad ^1H and ^{19}F NMR lines of the downstream and metal-free products as indicating their polymeric character. This is also consistent with their viscous (oily) character. **4**−**6**

HFIP: $CF_3\overset{\overset{O}{\|}}{C}CF_2H$ **4**

TFTB: $CH_3\overset{\overset{O}{\|}}{C}CF_2CH_3$ **5**

HFTB: $CF_3\overset{\overset{O}{\|}}{C}CF_2CH_3$ **6**

are the ketones expected to arise from γ-F abstraction followed by 1,2-R migration from $L_nMOCRR'CF_3$. Compounds **4** and **6** will have exceptionally electrophilic carbonyl carbons and be subject to polymerization to give **7** ($XOCRR'(-OCRR')_nY$; X and Y are end groups). Since the formerly ketonic carbons are now chiral, unselective polymerization will give stereochemically irregular polymers and broad NMR spectra. Since HFIP is unique among the OR_f substituents in giving an oily deposit immediately downstream from the furnace, it is apparent that ketone **4** has especially high reactivity. This we attribute to it being the only product with hydrogen directly attached to a carbon with three electron-withdrawing groups. Ketone **5** has few enough fluorines that it survives warming above −196 °C and was identified directly. Note that, when polymerization occurs, it could be catalyzed by trace HF produced during thermolysis.

Metal Fluoride Formation. The chemical vapor deposition of all the fluoroalkoxide species reported here produce predominantly metal fluorides rather than metal oxides as their solid-state products. The CVD process occurs within the short time that the precursor is in contact with the surface in the hot (furnace) zone, and the thermolysis reaction steps are influenced by the reactive sites on the growing film. These are both factors which could lead to kinetic control of product identity. However, the majority of our results give no evidence for kinetic constraints (direct M−O bonds in the precursor) being able to overcome the thermodynamic influence (MF_x is more thermodynamically stable than MO_y for sodium and zirconium)[7] on the deposition products. This could be taken to imply that merely having fluorine present in the precursor would result in the production of metal fluoride. There are examples

of kinetic control of CVD products for zirconium systems. Chemical vapor deposition studies of $Zr(TFAC)_4$ (TFAC = trifluoroacetylacetonate) and $Zr(HFAC)_4$ (HFAC = hexafluoroacetylacetonate) both produce metal oxides, not fluorides.[8] This may be due in part to the rigidity of the six-membered ring preventing any migration of fluorine to the metal during thermolysis. As noted earlier, we have also observed that CVD of a mixture of $Zr(O^tBu)_4$ and $Zr(TFTB)_4$ at 375 °C produced primarily metal oxide by X-ray diffraction. These results indicate that the production of metal fluoride is not merely due to fluorine being present in the precursor or the reactor system (e.g., as HF), suggesting the existence of a facile mechanism that works together with thermodynamics in those cases where fluorides are produced.

Initial evidence for such a mechanism was observed in the CVD studies of $Zr(TFTB)_4$. The production of 3,3-difluorobutan-2-one (a major volatile product) would result from the transfer of a fluorine to the metal center, in concert with the breaking of the zirconium–oxygen bond and a 1,2-methyl migration. The ketones expected from the other OR_f groups would be considerably more electrophilic and thus less stable. We observed secondary reactions upon warming the volatiles from −196 °C, which apparently consume these highly activated fluorinated species,[23] possibly via polymerization reactions:

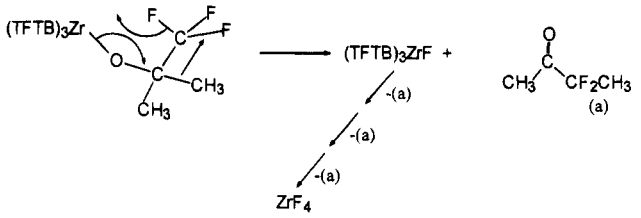

Evidence for the elimination of ketones was observed in the mass spectra of those $Zr(OR_f)_4$ systems which contain at least one viable migratory group (i.e., H or CH_3). For each of these steps, the corresponding metal fluoride species were detected. Thus, for $Zr(HFIP)_4$, the loss of pentafluoropropan-2-one (OC_3F_5H) is observed, Zr(TFTB) eliminates 3,3-difluorobutan-2-one ($OC_4F_2H_6$), and $Zr(HFTB)_4$ produces 1,1,1,3,3-pentafluorobutan-2-one ($OC_4F_5H_3$). For $Zr(PFTB)_4$, the formation of a metal fluoride species is detected, but multiple steps were not observed since the fragmentation seen in this system is less than that observed in other zirconium alkoxides. This clearly correlates with the low mobility of the CF_3 group.[24] Since mass spectral fragmentation via electron ionization has been shown to follow roughly thermolysis pathways,[16] the apparent elimination of ketone during mass spectral analysis is supporting evidence that this is a general mechanism for the production of metal fluorides from zirconium fluoroalkoxides.

The production of zirconium oxide via CVD thermolysis of fluoride free tetralkoxides is a facile process, occurring at temperatures as low as 350 °C.[2] The primary mechanism for this process involves γ-proton transfer.[2,25] Even though two of the four zirconium precursors examined here contain γ-hydrogens ($Zr(TFTB)_4$, $Zr(HFTB)_4$), this mechanism does not occur.

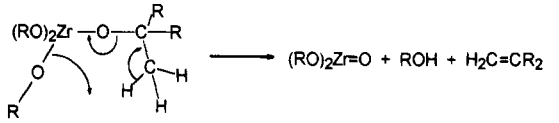

This is surprising, considering that the steric constriction of the transition state would be less than that of a fluoride transfer (six- vs five-membered ring), and that the C–H bond and the C–O bond are significantly weaker than the C–F bond (99, 88, and 114 kcal/mol, respectively). The lack of γ-hydrogen transfer in $Zr(TFTB)_4$ and $Zr(HFTB)_4$ can be attributed in part to electronic properties of the fluoroalkoxide group. For γ-hydrogen transfer, the alkoxy oxygen must be sufficiently Brønsted basic to accept the hydrogen and the C–O bond must be sufficiently weak to be cleaved. In fluoroalkoxides, the inductive effects of the CF_3 groups both reduce its Brønsted basicity and strengthen the C–O bond via hyperconjugation effects (lowering the energy of the σ* orbitals at the α-carbon, thus allowing for C–O multiple bonding character).[26] This effectively permits the fluorine-transfer process to dominate. These inductive effects are significant, even in the case of a TFTB group, where there is only one CF_3 group. The pK_a's of the free alcohols provide a good measure of the influence of the CF_3 group. There is a large increase of the Brønsted acidity (and a corresponding decrease of Brønsted basicity) with each successive CF_3 group (HO^tBu, pK_a = 18.6; H-TFTB, pK_a = 11.4; H-HFTB, pK_a = 9.6; H-PFTB, pK_a = 5.4).[27]

For the sodium-containing species, no such mechanistic information is available. Analysis of deposition volatiles indicated the likelihood of multiple products with the presence of secondary reactions in the volatiles trap for three of the four systems. Mass spectral analysis did not offer any insight since the primary fragmentation pattern involved the breaking up of the $Na(OR_f)$ oligomers.

Trends in deposition temperatures of the fluorinated precursors follow the changes in the steric bulk of the precursor ligands. With increasing size of the ligands (HFIP < TFTB < HFTB < PFTB), there is a corresponding increase in the temperature needed to initiate deposition (with the exception of $Zr(HFIP)_4$). The presence of very bulky ligands can interfere with the binding of the precursor to the substrate, a preliminary step in the deposition process.[28] Higher temperatures would be necessary to increase the rate of subsequent steps of thermolysis, so that they occur before the molecule desorbs from the surface. This hypothesis is supported by the correlation between the ability for the precursor metal center to bind external Lewis bases and deposition temperature. For the sodium alkoxides, *intermolecular* metal–fluorine contacts are observed in the solid-state structures of the two species with the lowest deposition temperatures ($[Na(HFIP)]_4$[9] and $[Na(TFTB)]_4$[29]), but these contacts are absent in $[Na(PFTB)]_4$, the species with the highest deposition temperature. In the zirconium systems, the molecular species are found to bind Lewis bases (amines)[9] indicat-

(23) Chambers, R. D. *Fluorine in Organic Chemistry*; John Wiley and Sons: New York 1973; Chapter 8.
(24) Chambers, R. D. *Fluorine in Organic Chemistry*; John Wiley and Sons: New York, 1973; Chapter 4.
(25) Sen, A.; Rhubright, D.; Nardi, M. *Inorg. Chem.* **1990**, *29*, 3065.
(26) Willis, J. C. *Coord. Chem. Rev.* **1988**, *88*, 133.
(27) In: *Ionization Constants of Organic Acids in Aqueous Solution*; Serjeant, E. P., Dempsey, B., Eds.; Pergamon Press: Oxford, 1979.
(28) Jensen, K. F.; Kern, W. In *Thin Film Processes II*; Vossen, J. L., Kern, W., Eds.; Academic Press: San Diego, 1991; p 283.
(29) As observed in the single-crystal X-ray studies of $[Na(TFTB)]_4$ and $[Na(PFTB)]_4$ (J. Samuels, unpublished results).

ing the availability of the metal center to surface active sites. While extensive studies of binding strength have not been made, intuitively one would expect the molecules with the greatest steric bulk to be least able to bind additional ligands.

The exception to this trend is $Zr(HFIP)_4$, which appears to have a significantly higher deposition temperature than expected (see results). The cause of this discrepancy may be due to this species having a greater molecular complexity than a simple monomer, thus increasing the overall steric bulk of the precursor. Evidence for this is found in the solution behavior of the molecule[9] as well as the presence of ions of larger mass than the parent ion in the mass spectrum.

A second explanation for the CVD behavior of these precursors is that deposition temperatures are a function of ease of R-group migration. In the case of $[Na(OR_f)]_4$, the lowest deposition temperature occurs for $[Na(HFIP)]_4$ (255 °C), which would require a hydrogen migration. In contrast, $[Na(TFTB)]_4$ requires a slightly higher thermolysis temperature (260 °C), and involves methyl migration. $[Na(HFTB)]_4$ (300 °C) also requires methyl migration, but *from* a significantly more electron deficient carbon (due to the electron withdrawing effects of the CF_3 groups). Finally, $[Na(PFTB)]_4$ requires a significantly higher temperature (400 °C) than the other sodium-containing precursors. This is likely due to the combination of removing a substituent *from* an electron-deficient carbon and the fact that the group migrating is CF_3. The zirconium species also follow this trend (Table 2) with the exception of $Zr(HFIP)_4$, which, as noted above, has a much higher deposition temperature than expected for a hydrogen migration. The cause of this discrepancy is unknown.

It is interesting to note that $[Na(HFIP)]_4$, $[Na(TFTB)]_4$, $[Na(HFTB)]_4$, and $Na_2Zr(HFIP)_6$ all deposit at significantly lower temperatures than the homometallic zirconium analogues. This reduction of deposition temperature can be attributed to the presence of intramolecular metal–fluorine contacts which were observed in the sodium-containing species but were absent in the $Zr(OR_f)_4$ precursors.[9] These contacts would have the effect of reducing the activation barrier for the fluoride-transfer step and correspondingly reduce the overall deposition temperature. This explains why the more electrophilic metal (Zr^{IV}) does not initiate CVD conversion (F abstraction) at lower temperatures than does Na^{I}.

The exception to the trend of reduced deposition temperature is $[Na(PFTB)]_4$. This species requires over 100 °C greater furnace temperatures for thermolysis. Since single-crystal X-ray diffraction studies have shown $[Na(PFTB)]_4$ to have intramolecular M–F contacts comparable to those observed in the other sodium-containing species,[9,29] the cause of the higher deposition temperature must be attributed to ligand steric bulk and poor migrating groups.

Alcohol Formation. Of significant interest is the presence of the parent alcohol in the volatiles of all the deposition studies, even though an alcohol is not one of the expected products for the proposed fluoride-transfer mechanism. It is our belief that the alcohol is the product of side reactions not involved in the formation of metal fluoride. For the formation of alcohol, a source of protons is necessary. While many of the precursor species contain hydrogen atoms which can be a source of the alcoholic proton, we and others[6] observe significant alcohol formation even from a totally fluorinated (i.e., hydrogen-free) molecule. This would indicate that the protons come from an external source (e.g., hydroxyl groups in the glass surface of the CVD reactor). These hydroxyls are likely to react with the precursor, resulting in binding of the metal to the surface and the elimination of alcohol:

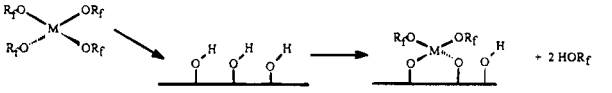

This process could occur at temperatures insufficient to allow the formation of metal fluoride, thus merely producing a layer of bound precursor, similar to the effect observed in the silylation of glass. Due to the large surface area of the reactor, significant amounts of alcohol would be produced. This process may be facilitated by the potentially greater electron donor ability of the oxide surface as compared to the fluoroalkoxide ligands,[26] stabilizing the electron-deficient metal center.

Conclusions

For all the above homoleptic fluoroalkoxide species, metal fluoride is the major solid-state CVD product. This product is independent of the metal present, degree of ligand fluorination, or the presence of metal–fluorine contacts in the precursor. On a more subtle level, the above parameters have a dramatic effect on deposition temperature. These observations will allow us to develop precursors to fluorine materials with lower deposition temperatures and hopefully cleaner films. We are also currently exploring the effects of deposition temperature and mixed ligand combinations on the CVD production of metal fluorides, which is relevant to sodium,[30] zirconium,[31] and other metal fluorides[32] as optical materials.

Acknowledgment. This work was supported by the Department of Energy. We thank F. R. Turner for electron micrography.

Supplementary Material Available: Tables of mass spectral data and a powder pattern of the CVD product from **2d** (6 pages). Ordering information is given on any current masthead page.

(30) Zwedowski, S.; Andrze, J. *Opt. Appl.* **1987**, *17*, 363.
(31) (a) Fujiura, K.; Nishida, Y.; Kobayashi, K.; Takahashi, S. *Optical Wave Guide Materials*; Broer, M. M., Sigel, G. H., Kersten, R. T., Kawazoe, H., Eds.; Materials Research Society Symposium Proceedings; Vol. 244, 1992. (b) Kono, T.; Morita, S.; Goto, T.; Nishiwaki, A. *Optical Wave Guide Materials*; Broer, M. M., Sigel, G. H., Kersten, R. T., Kawazoe, H., Eds.; Materials Research Society Symposium Proceedings, Vol. 244, 1992.
(32) (a) Izumituni, T.; Tokita, M.; Yamashita, T.; Miura, S. JPN Patent 62256740, 1986. (b) Harai, S.; Yoshiki, C., JPN Patent 63248737, 1988. (c) Korner, H. J. *Bull. Am. Phys. Soc.* **1988**, *33*, 1091.